THE JOURNAL OF BIOLOGICAL CHEMISTRY VOL. 289, NO. 44, pp. 30470–30480, October 31, 2014

Fibroblast Growth Factor Receptor 4 (FGFR4) Deficiency Improves Insulin Resistance and Glucose Metabolism under Diet-induced Obesity Conditions*

Received for publication, June 30, 2014, and in revised form, September 1, 2014 Published, JBC Papers in Press, September 9, 2014, DOI 10.1074/jbc.M114.592022

Hongfei Ge[‡1], **Jun Zhang**[‡1], **Yan Gong**[‡], **Jamila Gupte**[‡], **Jay Ye**[‡], **Jennifer Weiszmann**[‡], **Kim Samayoa**[‡], **Suzanne Coberly**[‡], **Jonitha Gardner**[‡], **Huilan Wang**[§], **Tim Corbin**[§], **Danny Chui**[§], **Helene Baribault**[‡], **and Yang Li**[‡2]

From [‡]*Amgen, Inc., South San Francisco, California 94080 and* [§]*Amgen, Inc., Thousand Oaks, California 91320*

Background: The role of FGFR4 in glucose and energy metabolism is not well defined.
Results: FGFR4-deficient mice display improved glucose metabolism and insulin sensitivity under high fat conditions.
Conclusion: These improvements are mediated in part by bile acid actions and induction of endocrine hormones.
Significance: FGFR4 antagonists alone, or in combination with other agents, could serve as a novel treatment for diabetes.

The role of fibroblast growth factor receptor 4 (FGFR4) in regulating bile acid synthesis has been well defined; however, its reported role on glucose and energy metabolism remains unresolved. Here, we show that FGFR4 deficiency in mice leads to improvement in glucose metabolism, insulin sensitivity, and reduction in body weight under high fat conditions. Mechanism of action studies in FGFR4-deficient mice suggest that the effects are mediated in part by increased plasma levels of adiponectin and the endocrine FGF factors FGF21 and FGF15, the latter of which increase in response to an elevated bile acid pool. Direct actions of increased bile acids on bile acid receptors, and other potential indirect mechanisms, may also contribute to the observed metabolic changes. The results described herein suggest that FGFR4 antagonists alone, or in combination with other agents, could serve as a novel treatment for diabetes.

Fibroblast growth factors (FGF)19 and FGF21 are two atypical members of the FGF family that have been recognized in recent years as novel hormones involved in the regulation of glucose, lipid, and energy metabolism (1–3). Both FGFs are members of a special subfamily of endocrine FGFs (4); they exhibit reduced affinity toward heparan sulfate proteoglycans and utilize a single-pass transmembrane protein, βKlotho, to activate FGF receptor signaling *in vitro* (5). FGFRs[3] are encoded by four genes, *Fgfr1*, *2*, *3*, *4*, and alternative splicing from *Fgfrs1–3* gives rise to *b* and *c* isoforms, resulting in a total of seven main receptors (6, 7). βKlotho interacts only with FGFR1c, 2c, 3c, and 4. Whereas FGF19 can activate all four βKlotho partner FGFRs, FGF21 activates βKlotho complexed with FGFR1c, 2c, 3c but not FGFR4 (8). Elucidating the roles of these four FGFRs, particularly in the context of FGF19 and FGF21, is an active area of research.

The reported pharmacological effects of FGF19 and FGF21 can be separated into three general categories: 1) both FGF19 and FGF21 similarly improve glucose disposal and reduce body weight; 2) FGF21 reduces plasma triglycerides (TG) and cholesterol, whereas the effects of FGF19 depends on the model tested and the duration of treatment (9); and 3) although FGF19 inhibits bile acid synthesis and reduces the bile acid pool, there is no report that FGF21 regulates bile acid metabolism (10, 2, 5). Because both FGF19 and FGF21 similarly activate βKlotho complexed with FGFR1c, 2c, and 3c, it is reasonable to speculate that one of the receptors alone, or combination with one another, are responsible for the similar effects of FGF19 and FGF21 on glucose and body weight regulation. Recent studies using several FGFR1c specific activators demonstrated similar beneficial effects to FGF21, whereas FGFR1 knock-out (KO) in mice abolished the ability of FGF21 to reduce glucose, body weight, TG, and cholesterol levels, thus establishing βKlotho/FGFR1c as the principal receptor complex in mediating the beneficial functions of these two endocrine FGFs on glucose, plasma lipids, and body weight (reviewed in Ref. 5).

The last βKlotho partner, FGFR4, can only be activated by FGF19 and not FGF21 (8, 11). FGFR4 is the predominant receptor expressed in the liver. FGF19-mediated activation of FGFR4 has been linked to regulation of bile acid homeostasis and plasma TG and cholesterol levels, the effects of which differentiate FGF19 from FGF21, as described above. It has been proposed that FGF19 is a farnesoid X receptor target gene (12). Postprandial increases in intestinal bile acid levels activate farnesoid X receptor in intestinal epithelia, which in turn induce expression and secretion of FGF19. Subsequently, FGF19 signals the liver to reduce bile acid synthesis by inhibiting expression of cholesterol 7α-hydroxylase (CYP7A1), the enzyme responsible for the rate-limiting step of bile acid synthesis, via activation of hepatic FGFR4, thus completing a negative feedback loop on bile acid synthesis (12). Consistent with this, FGFR4 KO mice exhibit increased *Cyp7a1* expression and bile acid pool size due to the inactivation of the FGF19/FGFR4 axis (10).

* All authors are Amgen, Inc. employees.
[1] Both authors contributed equally to this work.
[2] To whom correspondence should be addressed: Dept. of Metabolic Disorders, Amgen, Inc., 1120 Veterans Blvd., South San Francisco, CA 94080. Tel.: 650-244-2524; E-mail: yangl@amgen.com.
[3] The abbreviations used are: FGFR, FGF receptor; TG, triglyceride(s); CYP7A1, cholesterol 7α-hydroxylase; AAV, adeno-associated virus; OGTT, oral glucose tolerance test(s); ZFN, zinc finger nuclease; qRT-PCR, quantitative RT-PCR; BW, body weight; HFD, high fat diet.

In addition to its established role in regulating bile acid metabolism, reports suggest FGFR4 regulates glucose and energy metabolism; however, the data have been inconsistent. For example, preventing FGF19 to activate FGFR4 *in vivo* had no significant impact on the ability of FGF19 to regulate glucose (13), and FGFR4 KO mice still exhibited responsiveness to FGF19 in regulating glucose and body weight (14, 15). In addition, contrary to treatment with recombinant FGF19 or FGF21, acute treatment of an FGFR4-specific activator to diabetic mice did not affect plasma glucose levels (11). Thus, these results argue that FGFR4 plays a minimal role in mediating the effects of endocrine FGFs on regulating glucose homeostasis. However, given that FGFR4 is the predominant receptor expressed in the liver, a role for FGFR4 in the reported FGF19-mediated hepatic glycogen synthesis (16) and inhibition of hepatic gluconeogenesis (17) could not be ruled out.

The effects of FGFR4 in glucose and body weight regulation have also been addressed using a FGFR4 KO mouse model (18). Reportedly, FGFR4 KO mice exhibit worsened glucose disposal and increased adipose depot size. Because FGFR4 KO mice had increased bile acid synthesis, the worsening effect on glucose metabolism appears inconsistent with effects of bile acids to prevent hyperglycaemia and insulin resistance (19) and the beneficial effects on glucose metabolism in other situations of increased bile acid synthesis, such as from bile acid resin treatment (20) or in mice with defective intestinal bile acid transporter (21). Additionally, a recent study of liver-specific FGFR4 knockdown mice, using an antisense RNA approach, resulted in improvement in glucose metabolism, insulin sensitivity, and reduction in body weight (22). Therefore, the role for FGFR4 in glucose and body weight regulation remains to be defined.

To resolve these inconsistencies, we generated our own FGFR4 KO mice. Here, we report that the FGFR4 deficiency prevents high fat diet induced insulin resistance and glucose intolerance. Using these KO mice, we also confirm that the previously reported effects of FGF19 to increase plasma TG is mediated through FGFR4 (9). Potential mechanisms leading to these metabolic changes are discussed.

EXPERIMENTAL PROCEDURES

Animals and Treatments—All animal housing conditions and research protocols were approved by the Amgen Institutional Animal Care and Use Committee. Mice were housed in a specified-pathogen free, AAALAC (Association for Assessment and Accreditation of Laboratory Animal Care), international-accredited facility in ventilated microisolators. Procedures and housing rooms are positively pressured and regulated on a 12:12 dark/light cycle. FGFR4 KO mice and WT littermates were singly housed. They were initially fed standard chow (2020× Teklad global soy protein-free extruded rodent diet; Harlan) and received reverse-osmosis purified water *ad libitum* via an automatic watering system. When indicated, mice received a 60 kcal % high-fat diet (D12492, Research Diet).

For infusion studies, the indicated amounts of protein were delivered continuously using implanted Alzet miniature infusion pumps (100-μl model 1007D, Alzet). These pumps were implanted subcutaneously on the upper part of the back using aseptic technique while the animal was anesthetized with isoflurane. Feces were collected for 3 days post-pump implantation. Tissues were collected for bile acid pool measurement.

Recombinant adeno-associated virus (AAV) expressing FGF15 was produced by transient transfection into 293T cells using helper-free system, purified by gradient centrifugation, buffer exchanged. 1×10^{10}–3×10^{11} virus particles per mouse, containing a vector expressing FGF15 or an empty vector as negative control, were injected through the tail vein.

For studies with chronic protein injection, 9–11-week-old male mice were fed with a 60 kcal % fat diet (D12492, Research Diets) for 8 weeks. Two days before protein injection, mice were divided into two groups ($n = 12$) based on body weight and glucose. Starting from day 0, mice were intraperitoneally injected daily with recombinant FGF19 protein (at 1 mg/kg body weight in 0.2 ml of PBS) or same volume of PBS control. Oral glucose tolerance tests (OGTT) were performed following a 4-h fast. Terminal bleeding was performed following a 6-h fast.

FGFR4 KO Mouse Generation—FGFR4 KO mice were created using a pair of zinc finger nucleases (ZFNs) from Sigma-Aldrich targeting exon 8 of mouse FGFR4. ZFN binding sites are underlined below with a six-base pair (bp) spacer between the two sites (5′-CTGAGGAACGTGTCC**GCTGAG**GATGCAGGAGAGTATGACTCCTTGCACAGG**CGACTC**CTACGTCCTCTCATA-5′).

Design, cloning, and validation of the ZFNs were performed by Sigma-Aldrich. Messenger RNA (provided from Sigma-Aldrich) for each of the ZFNs were diluted in RNase-free microinjection buffer to a final concentration of 2.8 ng/μl for each ZFN (5.6 ng/μl total concentration). The ZFNs were microinjected into the pronucleus of fertilized one-cell embryos (0.5 days post coitus) obtained from the mating of C57BL/6 (Taconic) males to superovulated C57BL/6 (Taconic) female mice. Microinjected eggs were transferred to pseudopregnant Swiss Webster recipients. Founder pups were screened for ZFN induced mutations in FGFR4 by sequencing across exon 8. Two founders, one with a 2-bp deletion and the other with an 80-bp deletion were expanded for further analysis.

Expression Analysis of FGFR4 in Knock-out Mice—FGFR4 expression in the liver was analyzed using quantitative RT-PCR (qRT-PCR). Liver RNA was isolated from WT and FGFR4 KO mice using the Qiacube and standard Qiagen RNA isolation protocol. The primers used to detect the FGFR4 deletion were located spanning the 80-bp deletion and the primer probe sequences were 5′-GCAACTCCATCGGCCTTTCCTACCAG-3′, 5′-AGAACCAGTGAGCCTGATACATACAG-3′, and 5′-6FAM-AGCAACCCCTGAGGCCAGATACACAGATAT-BHQ1–3′. FGFR4 primers from ABI (Applied Biosystems, Mm01341852_m1 located in exon boundary 11–12) were also used. qRT-PCR was performed on the Stratagene Mx3000P quantitative PCR machine with the Stratagene Brilliant II qRT-PCR Master Mix Kit, 1-Step (600809, Stratagene) using 50 ng of RNA/well and normalized to mouse GAPDH (4352932E and 4352339E, ABI).

qRT-PCR—Tissue total RNA was isolated using QIAcube and RNeasy kit (Qiagen). All reactions were performed in duplicates on a Stratagene MX3000p sequence detection system or BioMark™ HD System, and relative mRNA levels were calculated by

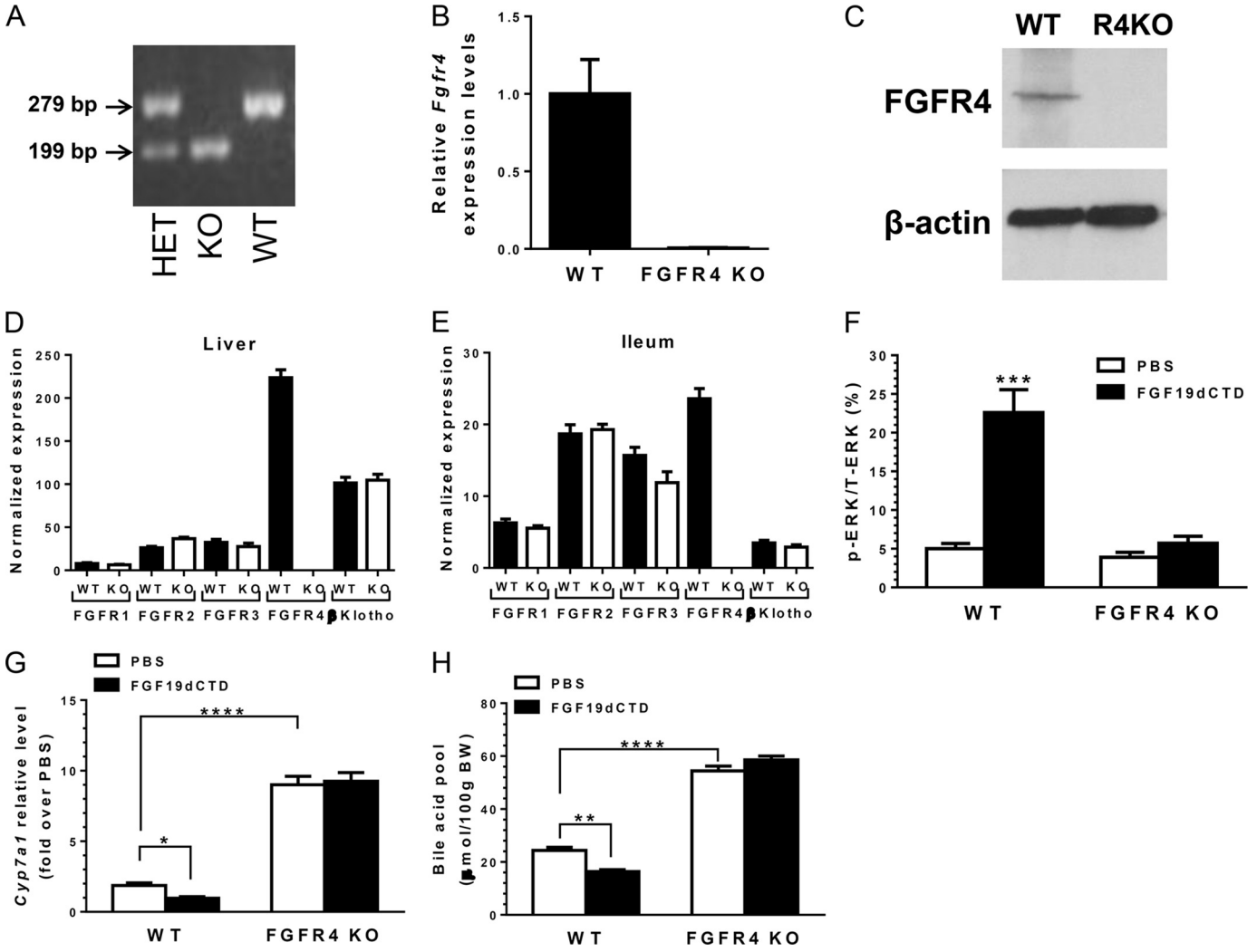

FIGURE 1. **FGFR4 80-bp deletion line lost FGFR4 expression and signaling.** *A*, genotyping characterization of the 80-bp deletion FGFR4 KO animals. A predicted 279-bp band in WT littermate control animals, 199 bp in KO animals, and both bands in heterozygous (*HET*) animals. *B*, qRT-PCR analysis of liver tissues showed the absence of wild type FGFR4 mRNA in FGFR4 KO animals compared with WT littermate controls ($n = 5$ each group). *C*, Western blotting detected FGFR4 specific band only in WT littermate liver but not in FGFR4 KO animals. Total protein lysate were mixed from four individual animals from each genotype and loaded in each lane. β-Actin was used as an internal loading control. *D* and *E*, qRT-PCR analysis of expression levels of *Fgfr1, Fgfr2, Fgfr3,* and *βKlotho* in comparison with *Fgfr4* from liver (*D*) and ileum (*E*) of wild type and FGFR4 KO animals ($n = 5$ each group). *F*, animals were treated with 1.5 mg/kg FGF19dCTD by intraperitoneal injection for 1 h. FGF19dCTD treatments significantly induced p-ERK signals in WT but not FGFR4 KO animals ($n = 6$ each group). *G* and *H*, FGF19dCTD were delivered chronically by Alzet pump with a speed of 1.5 mg/kg/day for 3 days. FGF19dCTD treatment suppressed liver *Cyp7a1* expression (*G*) and bile acid pool (*H*) only in WT but not KO animals ($n = 7–8$ each group). *, $p < 0.05$; **, $p < 0.01$; ***, $p < 0.001$; ****, $p < 0.0001$.

the comparative threshold cycle method using GAPDH as the internal control. The primer and probes sets used were as follows: *Fas* (Mm01204974_m1, ABI); *Ldlr*, (Mm00440169_m1, ABI); adiponectin (Mm01343606_m1, ABI); *Glut1* (Mm00441480_m1, ABI); leptin (Mm00434759_m1, ABI); *Pepck* (Mm00551411_m1, ABI); *G6p* (Mm04207417_m1, ABI); *Pc* (Mm00500992_m1, ABI); *Fgf21* (Mm.PT.56a.29365871.g, IDT(Integrated DNA Technologies)); *Cyp7a1* (Mm.PT.56a.17448793, IDT); *Hmgcr* (Mm.PT.56a.13325212, IDT); *Srebp1c* (Mm.PT.56a.42313188, IDT); *Fgf15* (Mm.PT.56a.32032431, IDT); *Slc10a2* (Mm.PT.56a.41743474, IDT); *Fgfr1* (Mm.PT.56a.13356831, IDT); *Fgfr2* (Mm.PT.56a.12775563, IDT); *Fgfr3* (Mm.PT.56a.12920207.g, IDT); and *βKlotho* (Mm.PT.56a.8497961, IDT).

Western Blotting—Livers from 8–10-week-old FGFR4 KO mice and age-matched WT littermates were collected and homogenized in lysis buffer (9803, Cell Signaling). 50 μg of total lysates were subjected to Western blot analysis using an anti-mouse FGFR4 (AF2265, R&D Systems) or anti-β-actin antibody (AB8229, Abcam). Secondary antibodies used were anti-goat IgG antibody conjugated with HRP (31402, Pierce) and anti-rabbit IgG antibody conjugated with HRP (7074, Cell Signaling).

ELISA—Microtiter plates were coated with 2.0 μg/ml of sheep anti-mouse FGF15 (AF76755, R&D Systems) or goat anti-mouse FGF21 (AF3057, R&D Systems) in PBS overnight at 4 °C. The plates were then blocked with 3% BSA in PBS overnight at 4 °C. Serum samples were diluted in PBS + 1% BSA and incubated for 1 h at room temperature and washed three times with PBS + 0.01% Tween 20. Biotinated antibodies in PBS + 1% BSA was added and incubated for 1 h at room temperature. Streptavidin-conjugated HRP was then added and incubated for 20 min. The plates were washed six times with PBS + 0.01% Tween 20 and developed with tetramethyl benzidine as substrate. 1 N HCl was added as the stop solution. The results were

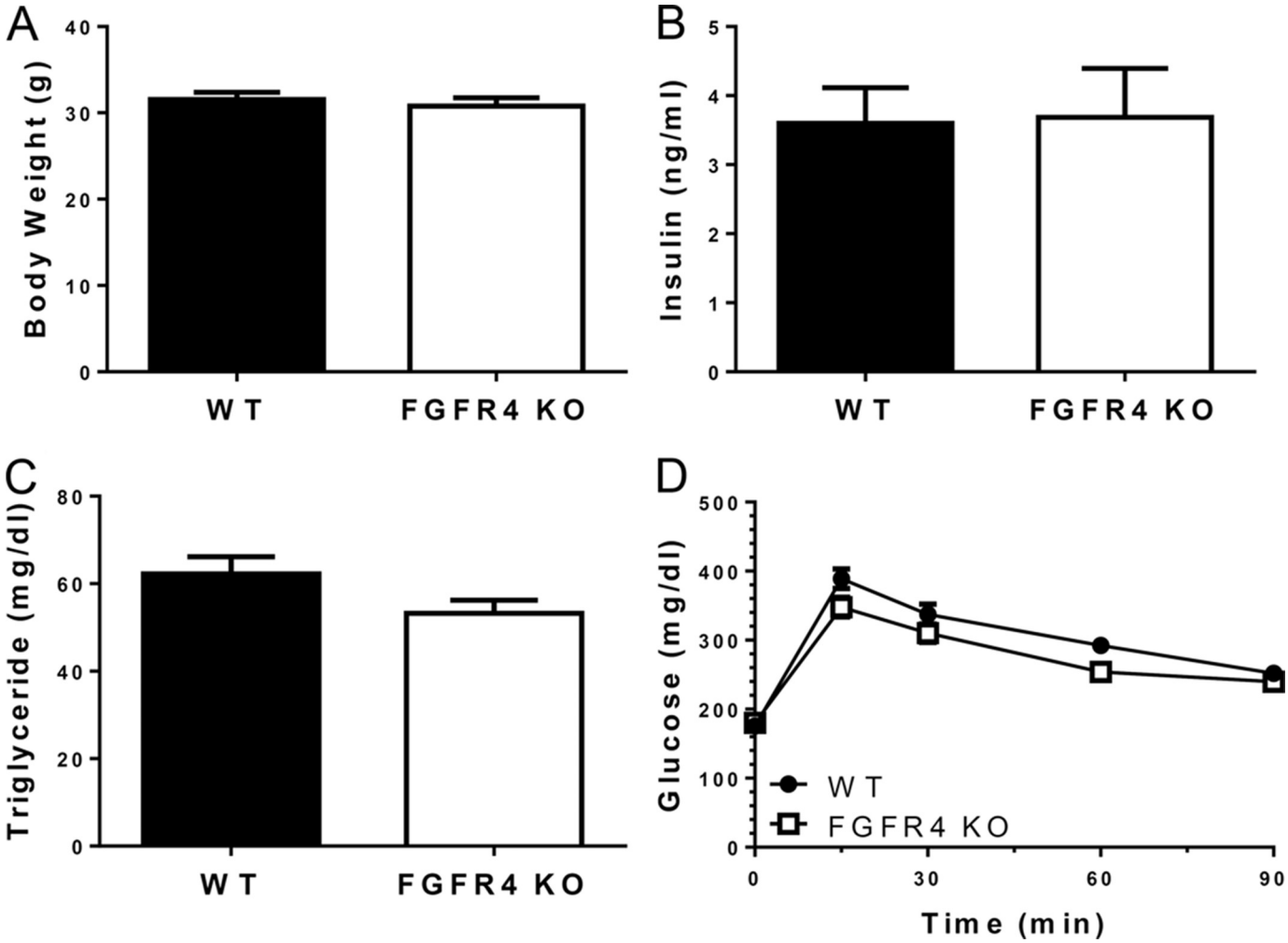

FIGURE 2. **Metabolic parameters were not significantly changed in FGFR4 KO animals upon chow diet feeding.** Body weight (*A*), serum insulin (*B*), serum triglyceride (*C*), and OGTT glucose response (*D*) were recorded from 13–14-week-old age-matched WT and KO animals ($n = 12$–13 each group). No significant differences were observed in all above parameter measured.

read on a SpecMax plate reader at 450 nm. Recombinant FGF15 and FGF21 (R&D Systems) were used for standard curve. Serum adiponectin was measured by Mouse Adiponectin Duo-Set ELISA kit (R&D Systems). Leptin level was measured with a mouse and rat leptin ELISA kit (Biovender).

MSD Analysis of Total and Phosphorylated ERK—Animals were treated with indicated reagents at indicated concentration for 1 h. Adipose tissue and liver were then harvested to prepare tissue lysates in lysis buffer (9803, Cell Signaling). 25 μl of cell lysate containing 1 μg of liver protein or 3 μg of fat protein was transferred to wells of phospho/total ERK1/2 whole cell lysate plates (K15107D, Meso Scale Discovery). Phosphorylated ERK (p-ERK) and total ERK were measured according to the manufacturer's protocol. Percent p-ERK in sample was determined using the formula provided by MSD for the multiplex assay format.

$$\%\ \text{Phosphorylated ERK} = \frac{2 \times \text{phosphorylated ERK}}{\text{phosphorylated ERK} + \text{total ERK}} \times 100 \quad \text{(Eq. 1)}$$

TABLE 1
A list of metabolic parameters measured in 13-week-old WT and FGFR4 KO animals upon regular chow diet feeding

	WT (mean ± S.E.)	KO (mean ± S.E.)	*p* value
	n = 12	*n* = 12	
Body weight (g)	31.5 ± 0.8	30.8 ± 0.9	0.553
Fast glucose (mg/dl)	176 ± 6	180 ± 11	0.718
Insulin (ng/ml)	3.6 ± 0.5	3.7 ± 0.7	0.922
Serum triglyceride (mg/dl)	62 ± 4	53 ± 3	0.083
Serum T-cholesterol (mg/dl)	172 ± 8	161 ± 5	0.225
Leptin (ng/ml)	5.6 ± 1.4	7.0 ± 1.7	0.529
Adiponectin (ng/ml)	5190 ± 164	5188 ± 194	0.992
Liver triglyceride (mg/g tissue)	9.2 ± 1.1	9.8 ± 0.6	0.657
MRI values			
Fat (g)	4.4 ± 0.4	5.0 ± 0.5	0.382
Lean (g)	20.7 ± 0.5	19.8 ± 0.3	0.102
Fluid (g)	3.6 ± 0.2	3.5 ± 0.1	0.683
% Fat	13.8 ± 1.0	15.9 ± 1.2	0.199
% Lean	65.8 ± 1.0	64.7 ± 1.2	0.480
% Fluid	11.4 ± 0.4	11.4 ± 0.2	1.000

Glucose Tolerance Tests and Plasma Insulin, Triglyceride, and Liver Triglyceride Measurements—Mice were fasted for 4 h beginning at 6 a.m. on the day of the experiment. Blood samples obtained from the tail vein were used for insulin and triglyceride measurements. Following administration of glucose (2 g per

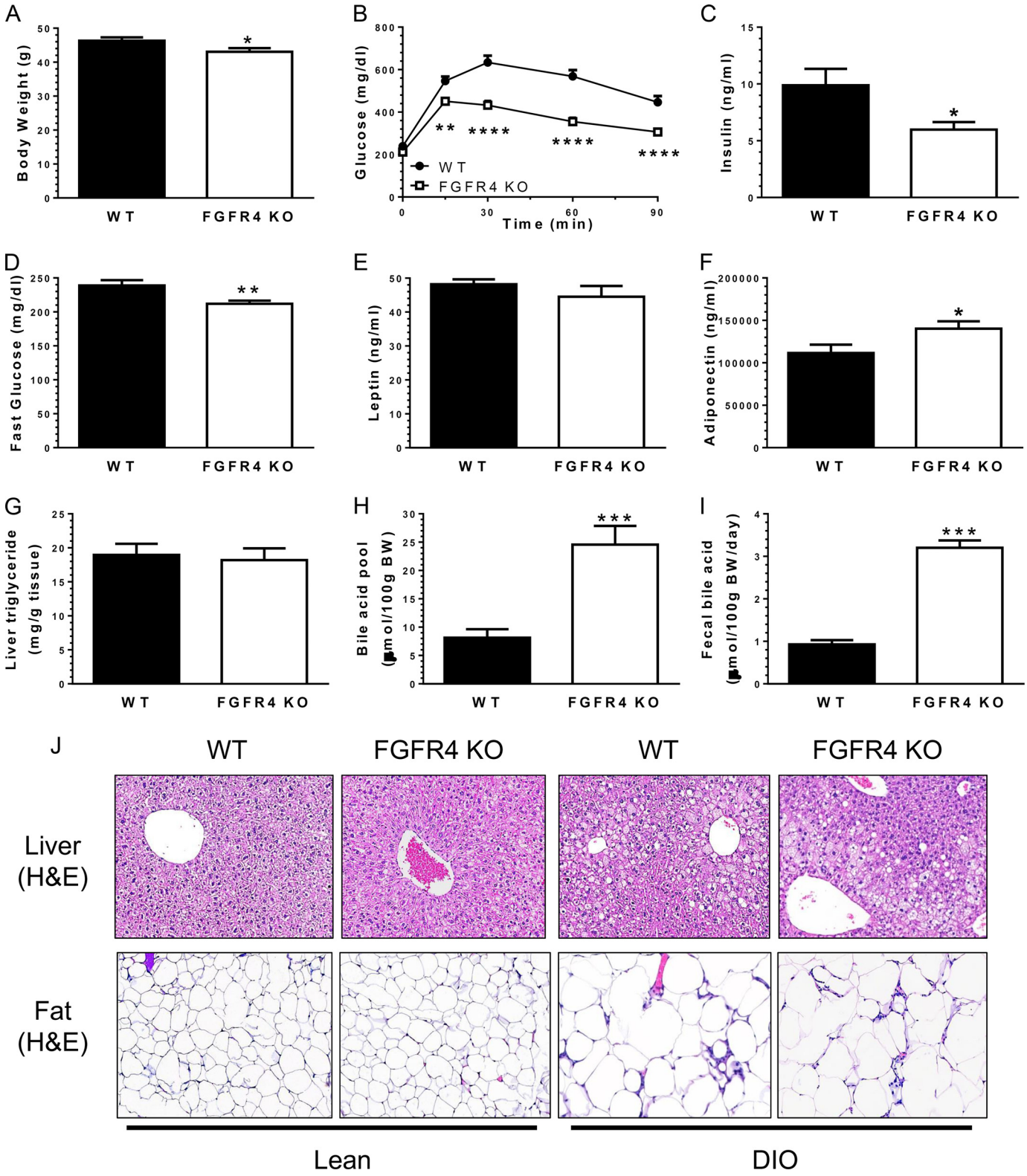

FIGURE 3. **Improved glucose metabolism and insulin sensitivity in FGFR4 KO animals upon high fat diet feeding.** 12-Week-old male WT and KO mice were fed with 60 kcal % high fat diet. Body weight (*A*), OGTT glucose response (*B*), serum insulin (*C*), and fasting glucose (*D*) were measured 8 weeks after high fat feeding, leptin (*E*), adiponectin (*F*), liver triglyceride (*G*), bile acid pool (*H*), and fecal bile acid levels (*I*) were measured 13 weeks after high fat feeding. (*, $p < 0.05$; ***, $p < 0.001$; ****, $p < 0.0001$; $n = 12$ each group). *J*, liver and fat H&E staining. Normal histology was observed in both WT and KO animals under normal chow conditions ($n = 12$). Upon high fat feeding, minimal/mild to severe hepatocyte vacuolation consistent with lipidosis was seen in the livers of both KO and WT groups and was similar between groups on average. White fat showed an increase in adipocyte size irregularity and inflammation in both KO and WT groups; the degree of change was again similar between groups. *DIO*, HFD induced obesity.

kg oral gavage), glucose levels were measured immediately before and 15, 30, 60, and 90 min after injection by using AlphaTrak blood glucose meter (Abbott). Plasma insulin content was determined by using Insulin (mouse) ultra-sensitive EIA kit (80-INSMSU-E10, ALPCO Diagnostics). Plasma TG was measure by using Infinity™ Triglyceride Reagent (TR22321, Thermo Scientific).

Feces and Tissue Pool Bile Acid Analysis—Bile acids were measured enzymatically using a bile acid quantification kit (BQ 092A-EALD, BQ Kits, Inc.). To determine fecal bile acid excretion, the feces from individually housed mice were collected over a 72-h period, dried, and weighed. Dried feces were then minced and extracted in 10 ml/g of 75% ethanol at ~50 °C for 2 h. The extract was centrifuged, and 1-ml samples of supernatant were diluted for assay to 4 ml with a 25% PBS solution. The bile acid concentration was measured enzymatically. The daily feces output (g/day per 100 g of body weight) and fecal bile acid content (μmol/g) were used to calculate the rate of bile acid excretion (μmol/day/100 g of body weight).

The total bile acid pool size was determined as bile acid content of the liver, the gallbladder, and the small intestine and its contents. After the mice were weighed, anesthetized, and exsanguinated, the fresh organs were collected, minced together, and extracted in 15 ml of 75% ethanol at ~50 °C for 2 h. The extract was centrifuged, 1-ml samples of supernatant for the assay were diluted to 4 ml with 75% ethanol, and then 1-ml samples were diluted to 4 ml with 25% PBS. Bile acids were determined enzymatically, and the pool size is expressed as micromoles of bile acid/100 g of body weight.

Tissue Histology Analysis—All collected tissues were prepared by fixing in 10% neutral buffered formalin for 24 h, processed to paraffin blocks, cut into 4-micron sections, and mounted onto glass microscope slides. The sections were dried overnight in a 37 °C oven, followed by a 1-h incubation in a 60 °C oven prior to deparaffinization. Deparaffinization and H&E staining (Surgipath, Buffalo Grove, IL) was performed on an automated multistainer (Leica ST 5020, Buffalo Grove, IL).

RESULTS

FGFR4 KO Generation and Characterization—FGFR4-specific KO lines were created using the ZFN technology. The ZFN cut site was located at GCTGAG inside exon 8, resulting in an 80-bp deletion founder line and a 2-bp deletion founder line. Both deletions created early stop codon in the extra cellular domain of FGFR4. Deletions were confirmed to be present in the germ line of both lines by sequencing the PCR amplified genomic region (data not shown). The phenotypes of the 2-bp deletion line are similar to the 80-bp deletion line (data not shown); the 80-bp deletion line is described from here on in the main text. Genotyping results of the 80-bp line showed the predicted 279-bp band in WT littermate control animals, 199 bp in KO animals, and both bands in heterozygous animals, demonstrating KO at the genomic level (Fig. 1*A*). This was further confirmed by qRT-PCR analysis using a forward primer within the 80-bp deletion region and reverse primer from the 3′ end outside of the 80-bp deletion. As shown in Fig. 1*B*, qRT-PCR of liver RNA samples did not detect any wild type message RNA from the FGFR4 KO mice. In addition, Western blotting analysis demonstrated the loss of the FGFR4 protein band at 110 kDa in liver total protein lysate from KO mice (Fig. 1*C*). To ensure that the FGFR4 KO is specific to FGFR4, we profiled the expression of *Fgfr1, 2, 3,* and *βKlotho* from liver and ileum and found no significant differences between WT and FGFR4 KO mice on the expression of these receptors (Fig. 1, *D* and *E*).

TABLE 2
A list of metabolic parameters measured in WT and FGFR4 KO animals upon 8 or 13 weeks (***) of high fat diet feeding (*, $p < 0.05$; **, $p < 0.01$)

	WT (mean ± S.E.)	KO (mean ± S.E.)	*p* value
	$n = 22$	$n = 26$	
Body weight (g)	46.3 ± 1.0	43.1 ± 1.1	**0.031***
Fast glucose (mg/dl)	239 ± 8	212 ± 5	**0.004****
Insulin (ng/ml)	9.9 ± 1.5	6.0 ± 0.7	**0.014***
Serum triglyceride (mg/dl)	50 ± 2	46 ± 2	0.171
Serum T-cholesterol (mg/dl)	188 ± 8	179 ± 6	0.395
Leptin (ng/ml)***	48.2 ± 1.4	44.5 ± 3.2	0.334
Adiponectin (ng/ml)***	3107 ± 221	4060 ± 217	**0.004****
Liver triglyceride (mg/g tissue)***	19.0 ± 1.6	18.2 ± 1.7	0.749
MRI values***			
Fat (g)	16.1 ± 0.4	16.5 ± 0.6	0.591
Lean (g)	21.6 ± 0.9	20.1 ± 0.5	0.119
Fluid (g)	5.4 ± 0.2	5.2 ± 0.3	0.628
% Fat	31.9 ± 0.7	33.9 ± 0.7	0.061
% Lean	42.7 ± 1.6	41.6 ± 1.1	0.593
% Fluid	10.6 ± 0.4	10.7 ± 0.6	0.908

To further confirm the loss of FGFR4 function in the animals, we injected the KO and WT age-matched littermate controls with FGF19dCTD (C-terminal deleted FGF19 protein), which was described previously as an FGFR4-specific activator (11). Injection of FGF19dCTD activated FGF signaling in the liver, as detected by increased phosphorylated ERK (p-ERK) levels in WT mice (Fig. 1*F*). However, this effect was completely abolished in FGFR4 KO animals. The effects of FGFR4 KO on bile acid regulation were further assessed. Similar to previously described FGFR4 KO mice, our FGFR4 KO mice showed increases in *Cyp7a1* expression and in bile acid pool levels compared with WT littermates (Fig. 1, *G* and *H*). FGF19dCTD treatment significantly suppressed *Cyp7a1* expression in the liver of WT mice, but this suppression was not observed in FGFR4 KO animals (Fig. 1*G*). Similar to the *Cyp7a1* expression pattern, FGF19dCTD treatment decreased bile acid pool only in WT, but not in FGFR4 KO mice (Fig. 1*H*). Thus, these results together demonstrate that our FGFR4 KO mice are indeed functional FGFR4 KOs.

FGFR4 KO Mice Display Significant Improvement in Glucose Metabolism and Insulin Sensitivity—FGFR4 KO mice appeared normal with no discernable differences to WT littermates. Despite an increase in bile acid synthesis and pool size (Fig. 1, *G* and *H*), on a normal chow diet FGFR4 KO mice displayed similar metabolic parameters to WT mice with respect to body weight (BW), plasma insulin, cholesterol, leptin, adiponectin, and slight trended reduction in plasma TG and in OGTT (Fig. 2 and Table 1). No difference in fat mass was observed, and histological analysis of both the adipose tissue and liver revealed no significant differences to WT mice (Table 1 and Fig. 3*J*).

However, after consumption of a high fat diet (HFD), loss of FGFR4 appeared to protect FGFR4 KO mice from HFD-induced insulin resistance and impaired glucose metabolism. Compared with WT mice on HFD, FGFR4 KO mice exhibited

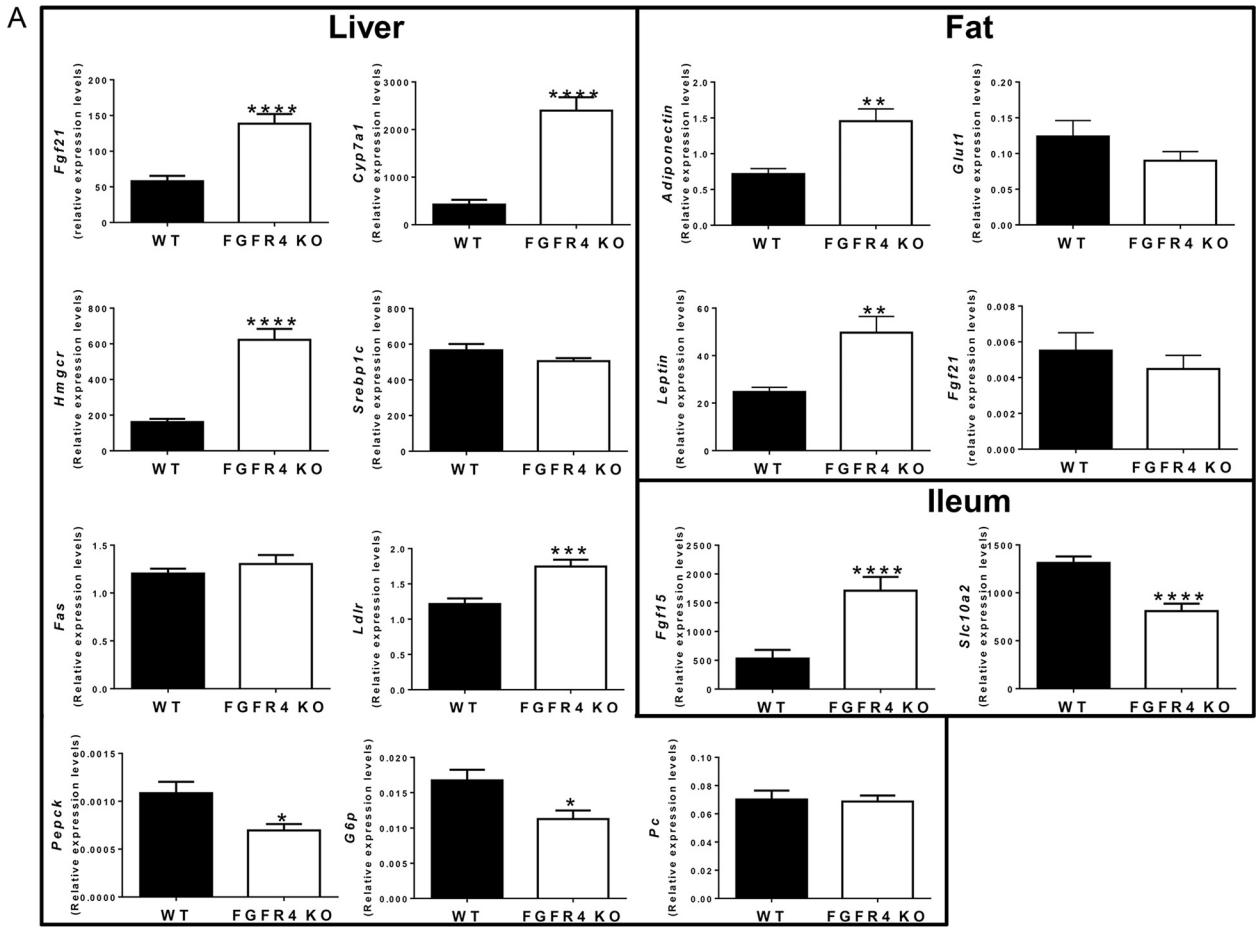
A
Liver
Fat
Ileum
Fgf21
Cyp7a1
Adiponectin
Glut1
Hmgcr
Srebp1c
Leptin
Fgf21
Fas
Ldlr
Fgf15
Slc10a2
Pepck
G6p
Pc
(Relative expression levels)
WT
FGFR4 KO

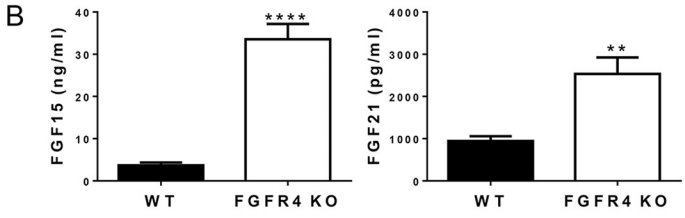
B
FGF15 (ng/ml)
FGF21 (pg/ml)
WT
FGFR4 KO

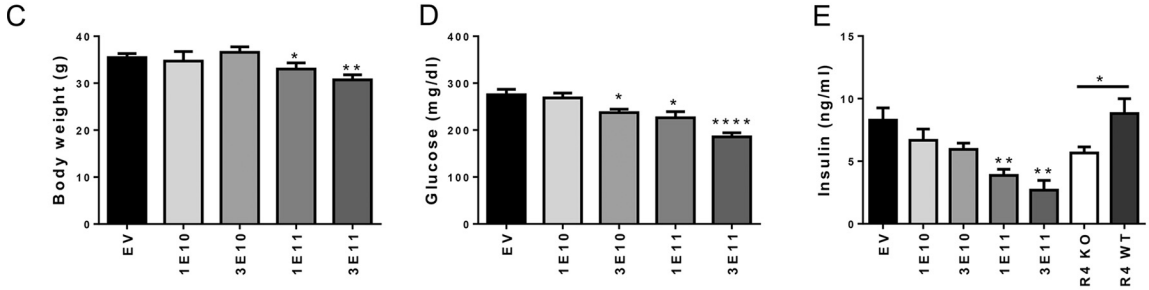
C
Body weight (g)
D
Glucose (mg/dl)
E
Insulin (ng/ml)
EV
1E10
3E10
1E11
3E11
R4 KO
R4 WT

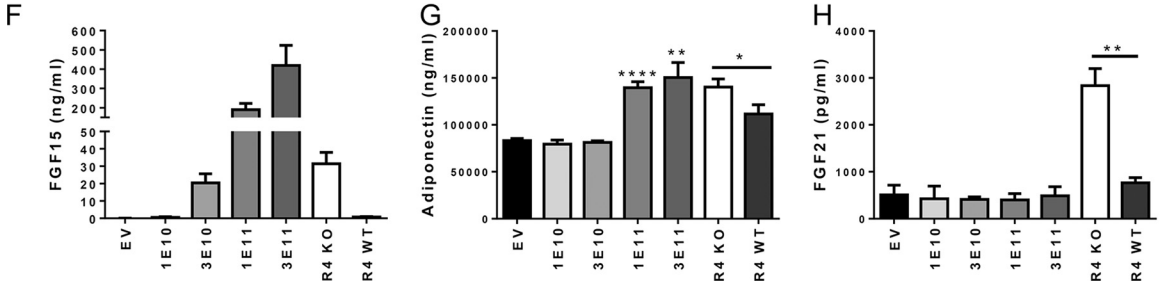
F
FGF15 (ng/ml)
G
Adiponectin (ng/ml)
H
FGF21 (pg/ml)
EV
1E10
3E10
1E11
3E11
R4 KO
R4 WT

significantly reduced plasma insulin levels and fasting glucose levels and a significant improvement in oral glucose tolerance (Fig. 3, *B–D*). Additionally, FGFR4 KO showed significantly increased plasma adiponectin levels (Fig. 3*F*). A small but significant reduction in BW was observed at week 8 post-high fat feeding (Fig. 3*A*). There were also trended reductions in cholesterol, leptin, and TG levels in KO mice; however, the changes in these parameters did not reach statistical significance (Fig. 3 and Table 2). Histological analysis of both the adipose tissue and liver revealed no significant differences to WT mice (Fig. 3*J*).

FGFR4 KO Mice Display Elevated Levels of Adiponectin, FGF15, and FGF21—To understand the underlying mechanism contributing to the observed changes in FGFR4 KO mice, we profiled expression of several key genes involved in lipid and glucose metabolism from liver, fat, and intestine. Consistent with the lack of significant changes to TG levels in the liver and plasma, no significant changes were noted for *Srebp1c* (sterol regulatory element-binding protein 1c) and *Fas* (fatty acid synthase) mRNA levels in the liver (Fig. 4*A*). In contrast, genes involved in cholesterol and bile acid metabolism were significantly changed in FGFR4 KO mice. Similar to mice fed a normal chow diet, HFD FGFR4 KO mice displayed significantly increased expression of liver *Cyp7a1* (Fig. 4*A*), indicating increased bile acid synthesis, as reflected by the increased bile acid pool and amount of fecal bile acids (Fig. 3, *H* and *I*). The cholesterol synthetic gene, *Hmgcr* (3-hydroxy-3-methyl-glutaryl-CoA reductase), and uptake gene, low density lipoprotein (LDL) Receptor (*Ldlr*) were both up-regulated in the liver of FGFR4 KO mice (Fig. 4*A*), which may be the consequence of increased demand for cholesterol to supply bile acid synthesis. To compensate for the overproduction of bile acids and increased bile acid pool size, the apical sodium-dependent bile acid transporter (*Slc10a2*) responsible for bile acid reabsorption in ileum was significantly reduced in FGFR4 KO mice (Fig. 4*A*).

The increased bile acid levels in the intestinal track also induced increased expression of fibroblast growth factor 15 (*Fgf15*, the mouse ortholog of human *FGF19*) in the ileum (Fig. 4*A*). Increased *Fgf21* expression in the liver of FGFR4 KO mice was also observed. Additionally, adiponectin expression was increased in fat tissues (Fig. 4*A*), consistent with the observed increase in plasma adiponectin protein levels (Fig. 3*F*). Although plasma leptin levels were not changed, its mRNA in fat was also increased (Fig. 4*A*). Liver expressions of *Pepck* and *G6p* were reduced consistent with improved glucose levels. Fat expression of *Fgf21*, *Glut1*, and liver *Pc* were not changed (Fig. 4*A*). Plasma levels of FGF15 and FGF21 were also measured and both were found to have increased in FGFR4 KO mice, consistent with the increase mRNA levels seen in ileum and liver (Fig. 4*B*). FGF15 plasma levels reached >30 ng/ml in FGFR4 KO mice (Fig. 4*B*) because a similar level of FGF19 or FGF21 could directly induce an improvement in glucose metabolism in our previously studies, we wondered whether this change in FGF15 could be the main contributor to the observed improvement in glucose metabolism in the FGFR4 KO mice. To test this, we injected HFD-fed WT mice with AAV-expressing FGF15. A dose-dependent reduction in BW, plasma glucose levels, and plasma insulin levels were observed with increasing amounts of viral injection indicating improvement in glucose metabolism and insulin sensitivity (Fig. 4, *C–E*). Plasma levels of FGF15 protein dose dependently increased with increasing viral injection (Fig. 4*F*). The group injected with 3×10^{10} viral particles displayed a plasma FGF15 level closely matching the level seen in FGFR4 KO mice (Fig. 4*F*). Similar to the phenotype observed in FGFR4 KO mice, this group displayed an improved glucose levels but without a robust BW reduction (Fig. 4, *C* and *D*). Adiponectin levels were also measured. Although a similar adiponectin levels were seen in higher FGF15 dose groups compared with FGFR4 KO mice, this increase was not apparent yet in the 3×10^{10} group (Fig. 4*G*). This suggests that FGF15 can induce adiponectin expression but the differences seen compared with KO mice might be due to duration of FGF15 exposure, as the AAV study was performed over only a 2-week period in contrast to the FGFR4 KO mice that were ~6 months old. FGF21 levels were also measured and no significant increases were seen in the AAV FGF15-injected groups. These results together suggest that although FGF15 might not account for all the changes observed in FGFR4 KO mice, the improvement in glucose metabolism seen in FGFR4 RO mice is likely primarily due to the increased FGF15 levels.

FGFR4 KO Mice Remain Responsive to FGF19 Treatment—Data in Fig. 4, *C–F*, suggest that the plasma level of FGF15 seen in FGFR4 KO mice has not reached the level that could induce the maximal metabolic changes; therefore, we wondered whether these animals could still respond to FGF19 treatment. 9–11-Week-old male mice were first put on HFD for 8 weeks. Similar to results shown in Fig. 3*B*, FGFR4 KO mice displayed significant improvements in an OGTT compared with WT littermates (Fig. 5*A*). Mice were then injected intraperitoneally with FGF19 daily for an additional 9 days. As shown in Fig. 5*B*, FGF19 treatment induced significant improvements in OGTT in WT mice. Despite an already improved response to a glucose challenge in FGFR4 KO mice, FGF19 further improved OGTT in these animals (Fig. 5*C*). FGF19 treatment also significantly reduced BW and fasting glucose levels in both WT and FGFR4 KO mice (Fig. 5, *D* and *F*), although effects on cholesterol and plasma insulin levels were not as pronounced in this study (Fig. 5, *G* and *H*).

Consistent with our previous report that FGF19 injection increased plasma TG levels (9), we observe a similar response to FGF19 injection in the WT group in the current study. Interestingly, the increase in plasma TG post-FGF19 treatment was abolished in FGFR4 KO mice (Fig. 5*E*). In the current study,

FIGURE 4. **Expression analysis of genes involved in metabolic regulations from liver, fat, and ileum.** *A*, qRT-PCR analysis of liver, fat, and ileum total RNA samples from both WT and KO animals ($n = 12–13$ each group). *B*, serum levels of FGF15 and FGF21 in WT and KO animals ($n = 12–13$ each group). *C–E*, body weight (*C*), glucose (*D*), and insulin (*E*) comparison between DIO mice injected with increasing doses of AAV expressing FGF15 or control AAV (*EV*) at week 2 post-AAV injection. *F–H*, serum exposure of FGF15 (*F*), adiponectin (*G*), and FGF21 (*H*) at week 2 post-AAV injection ($n = 7–8$). X-axis indicates the amount of viral particles injected, and FGFR4 KO and WT (*R4 KO* and *R4 WT*) were included as references. *, $p < 0.05$; **, $p < 0.01$; ***, $p < 0.001$; ****, $p < 0.0001$. *1E10*, 1×10^{-10}; *3E10*, 3×10^{-10}; *1E11*, 1×10^{11}; *3E11*, 3×10^{-11}. *DIO*, HFD induced obesity. *EV*, empty vector.

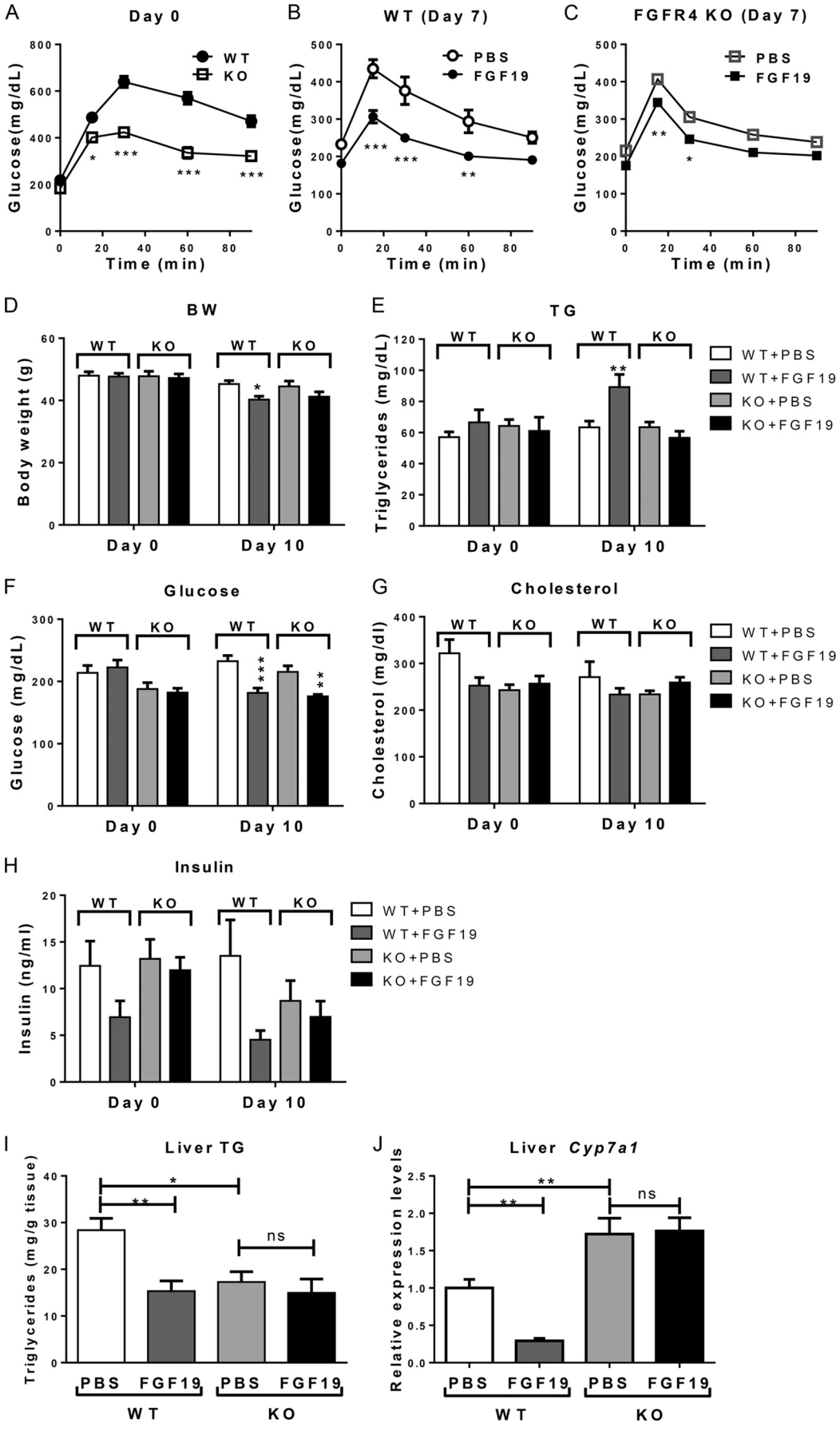
A
Day 0
WT
KO
Glucose(mg/dL)
Time (min)
B
WT (Day 7)
PBS
FGF19
Glucose(mg/dL)
Time (min)
C
FGFR4 KO (Day 7)
PBS
FGF19
Glucose(mg/dL)
Time (min)
D
BW
Body weight (g)
WT
KO
Day 0
Day 10
E
TG
Triglycerides (mg/dL)
WT+PBS
WT+FGF19
KO+PBS
KO+FGF19
F
Glucose
Glucose (mg/dL)
G
Cholesterol
Cholesterol (mg/dl)
H
Insulin
Insulin (ng/ml)
I
Liver TG
Triglycerides (mg/g tissue)
ns
PBS
FGF19
J
Liver Cyp7a1
Relative expression levels

HFD feeding resulted in an increase in liver TG content in WT mice, whereas lower TG content in the livers of KO mice suggest FGFR4 deficiency may be protective (Fig. 5*I*). FGF19 treatment reduced liver TG content in the WT mice; however, no further reduction was seen in FGFR4 KO in response to FGF19 injection (Fig. 5*I*). Finally, as established previously by many other laboratories, FGF19 injection suppressed liver *Cyp7a1* expression. FGFR4 KO mice displayed an elevated basal *Cyp7a1* levels compared with WT mice, and they also lost the ability to respond to FGF19 to suppress its expression (Fig. 5*J*).

DISCUSSION

Multiple FGF molecules have been shown to play important roles in regulating glucose, lipid, and energy homeostasis. Accordingly, understanding which FGF receptors are responsible for these activities is important to not only elucidate the signaling pathways for mechanism studies but also to devise appropriate strategies for potential therapeutic development. The role of FGFR4 in regulating bile acid synthesis is well defined, FGF15/FGF19 activate liver FGFR4 to suppress *Cyp7a1* expression and bile acid synthesis, whereas FGFR4 deficiency leads to increase bile acid synthesis and bile acid pool size (10). Our studies replicated these previous findings. Consistently, our FGFR4 KO mice showed increased *Cyp7a1* expression in the liver, and the increased bile acid synthesis was reflected by the increased bile acid pool size and increased excretion of bile acids in feces under both lean and obese conditions (Figs. 1, 3, and 5). The demand for cholesterol from increased bile acid synthesis may also account for the observed increases in cholesterol synthesis and uptake into hepatocytes as the expression of both *Hmgcr* and *Ldlr* were significantly increased (Fig. 4). As a potential compensatory mechanism to limit bile acid exposure induced toxicity, the major bile acid transporter, *Slc10a2*, in the ileum was reduced.

The increased bile acid pool size and flux in the intestine also resulted in a dramatic induction of *Fgf15* expression in the ileum. Correlating with this induction, plasma levels of FGF15 increased several hundred fold from the normal pg/ml quantities to >30 ng/ml in FGFR4 KO mice (Fig. 4). Liver *Fgf21* expression and plasma FGF21 levels were also increased, although to a much lesser extent than FGF15 (Fig. 4). This induction may come from both bile acid induced farnesoid X receptor activation and FGF15 action in the liver as reported previously (23). Adiponectin expression from fat and plasma adiponectin levels were also increased significantly (Fig. 4). We believe these changes, together, contributed to the improvement in glucose metabolism, insulin sensitivity, and reduction in body weight observed in HFD FGFR4 KO mice (Fig. 6). Despite the dramatic induction in FGF15 levels, significant body weight reduction was only observed in one HFD study. This is consistent with the dose response studies with AAV delivered FGF15 (Fig. 4) where plasma exposures in the 30 ng/ml range, although several hundred folder higher than normal levels, is not yet high enough to consistently affect body weight. This also explains why FGFR4 KO mice can still respond to additional FGF19 in both our studies and others (Fig. 5) (14, 15). Because our FGFR4 KO is systemic KO, we cannot rule out whether the lack of FGFR4 expression in tissues other than liver also contributes to the observed metabolic phenotype. Generation of a liver specific FGFR4 KO mouse line in the future could help to provide more definitive answers. But taken together, our data suggest that the induction of various endocrine molecules, in particular, the induction of FGF15 from ileum due to liver FGFR4 deficiency is the main contributor to the observed improvements in glucose metabolism.

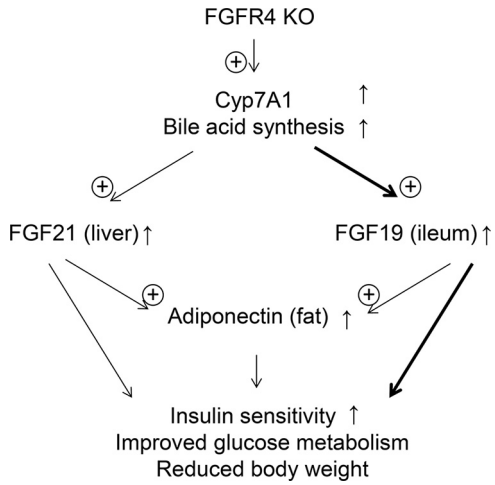

FIGURE 6. **A model of FGFR4-mediated metabolic regulations.** FGFR4 regulates bile acid synthesis by suppressing expression of *Cyp7a1*, the bile acid-producing enzyme in liver. In FGFR4 KO, increased basal bile acid synthesis triggered up-regulation of FGF21 in liver and FGF19/FGF15 in ileum. Adiponectin is also increased in the adipose tissue. The endocrine factors together contribute to the improvements in glucose response, insulin sensitivity, and body weight. The FGF19/FGF15 pathway is probably the main contributor to these metabolic changes as depicted by *thicker lines*.

Our finding that FGFR4 KO mice exhibit improved glucose metabolism and insulin sensitivity is in complete contrast to a previous FGFR4 KO study (18). In the previous study, FGFR4 KO mice displayed expanded fat tissues, worsened glucose handling, reduced insulin sensitivity, increased plasma TG and cholesterol levels, but had improved liver steatosis (18). Our FGFR4 KO mice did not show expanded fat mass (Figs. 2 and 3), and TG levels showed either no significant change or lowering compared with WT mice (Fig. 5). The differences in genetic backgrounds and how the KO construct were designed could contribute to the observed differences. Our findings, however, are consistent and supported by several lines of evidence. First, we generated two independent mouse lines, and both showed similar effects in improving glucose metabolism. Second, a recent report of FGFR4 knockdown in mice using an antisense RNA approach also described improvements in glucose metab-

FIGURE 5. **FGFR4 KO mice maintained response to FGF19 treatment induced changes in glucose and insulin regulation.** 9–11-week-old male WT and KO mice were fed with 60 kcal % high fat diet for 8 weeks. *A*, OGTT responses of WT and FGFR4 KO animals ($n = 25$ each group). *B–J*, WT and FGFR4 KO animals were further divided into two groups. PBS and 1 mg/kg FGF19 were injected intraperitoneal daily for 9 days. *B* and *C*, at day 7, FGF19 treatment improved OGTT responses in both WT (*B*) and FGFR4 KO (*C*) animals. *D–J*, at day 10 when the study was terminated, body weight, serum TG, fast glucose, serum cholesterol, insulin, liver TG, and liver *Cyp7a1* expression were measured. *, $p < 0.05$; **, $p < 0.01$; ***, $p < 0.001$; *ns*, no significance.

olism and insulin sensitivity and a strong reduction in body weight (22). Although it is difficult to rule out the body weight effects might be due to off-target actions or more restricted effects on liver FGFR4 expression from antisense approach, their observation of glucose improvement is consistent with our findings. Third, an increase in bile acids has been reported to prevent hyperglycaemia and insulin resistance in rodents (19); in addition, we observe bile acid-induced increases in FGF15, FGF21, and adiponectin levels, all of which may contribute to improved glucose metabolism and insulin sensitivity.

In conclusion, we show that FGFR4 deficiency in mice leads to improved glucose metabolism and insulin sensitivity. We propose that this improvement is mediated indirectly through the increased bile acid pool-induced increases in endocrine FGF factors, adipocytokines, and perhaps direct actions of bile acids on bile acid receptors. These studies raise the exciting possibility to evaluate whether FGFR4 antagonists alone or in combination with other agents could serve as novel treatments for diabetes.

Acknowledgments—We thank Jay Tang, Bryan Lemon, Ning Sun, Ki Jeong Lee, and Allison Whalen for technical assistance; William Richards and Scott Simonet for helpful discussions; and Ingrid Rulifson for editing this manuscript.

REFERENCES

1. Zhao, Y., Dunbar, J. D., and Kharitonenkov, A. (2012) FGF21 as a therapeutic reagent. *Adv. Exp. Med. Biol.* **728,** 214–228
2. Potthoff, M. J., Kliewer, S. A., and Mangelsdorf, D. J. (2012) Endocrine fibroblast growth factors 15/19 and 21: from feast to famine. *Genes Dev.* **26,** 312–324
3. Angelin, B., Larsson, T. E., and Rudling, M. (2012) Circulating fibroblast growth factors as metabolic regulators–a critical appraisal. *Cell Metab.* **16,** 693–705
4. Kuro-o, M. (2012) Klotho and βKlotho. *Adv. Exp. Med. Biol.* **728,** 25–40
5. Zhang, J., and Li, Y. (2014) Fibroblast growth factor 21, the endocrine FGF pathway and novel treatments for metabolic syndrome. *Drug Discov. Today* **19,** 579–589
6. Plotnikov, A. N., Hubbard, S. R., Schlessinger, J., and Mohammadi, M. (2000) Crystal structures of two FGF-FGFR complexes reveal the determinants of ligand-receptor specificity. *Cell* **101,** 413–424
7. Johnson, D. E., and Williams, L. T. (1993) Structural and functional diversity in the FGF receptor multigene family. *Adv. Cancer Res.* **60,** 1–41
8. Kurosu, H., Choi, M., Ogawa, Y., Dickson, A. S., Goetz, R., Eliseenkova, A. V., Mohammadi, M., Rosenblatt, K. P., Kliewer, S. A., and Kuro-o, M. (2007) Tissue-specific expression of βKlotho and fibroblast growth factor (FGF) receptor isoforms determines metabolic activity of FGF19 and FGF21. *J. Biol. Chem.* **282,** 26687–26695
9. Wu, X., Ge, H., Baribault, H., Gupte, J., Weiszmann, J., Lemon, B., Gardner, J., Fordstrom, P., Tang, J., Zhou, M., Wang, M., and Li, Y. (2013) Dual actions of fibroblast growth factor 19 on lipid metabolism. *J. Lipid Res.* **54,** 325–332
10. Jones, S. A. (2012) Physiology of FGF15/19. *Adv. Exp. Med. Biol.* **728,** 171–182
11. Wu, X., Ge, H., Lemon, B., Weiszmann, J., Gupte, J., Hawkins, N., Li, X., Tang, J., Lindberg, R., and Li, Y. (2009) Selective activation of FGFR4 by an FGF19 variant does not improve glucose metabolism in ob/ob mice. *Proc. Natl. Acad. Sci. U.S.A.* **106,** 14379–14384
12. Holt, J. A., Luo, G., Billin, A. N., Bisi, J., McNeill, Y. Y., Kozarsky, K. F., Donahee, M., Wang, D. Y., Mansfield, T. A., Kliewer, S. A., Goodwin, B., and Jones, S. A. (2003) Definition of a novel growth factor-dependent signal cascade for the suppression of bile acid biosynthesis. *Genes Dev.* **17,** 1581–1591
13. Ge, H., Baribault, H., Vonderfecht, S., Lemon, B., Weiszmann, J., Gardner, J., Lee, K. J., Gupte, J., Mookherjee, P., Wang, M., Sheng, J., Wu, X., and Li, Y. (2012) Characterization of a FGF19 variant with altered receptor specificity revealed a central role for FGFR1c in the regulation of glucose metabolism. *PLoS One* **7,** e33603
14. Fu, L., John, L. M., Adams, S. H., Yu, X. X., Tomlinson, E., Renz, M., Williams, P. M., Soriano, R., Corpuz, R., Moffat, B., Vandlen, R., Simmons, L., Foster, J., Stephan, J. P., Tsai, S. P., and Stewart, T. A. (2004) Fibroblast growth factor 19 increases metabolic rate and reverses dietary and leptin-deficient diabetes. *Endocrinology* **145,** 2594–2603
15. Wu, A. L., Coulter, S., Liddle, C., Wong, A., Eastham-Anderson, J., French, D. M., Peterson, A. S., and Sonoda, J. (2011) FGF19 regulates cell proliferation, glucose and bile acid metabolism via FGFR4-dependent and independent pathways. *PLoS One* **6,** e17868
16. Kir, S., Beddow, S. A., Samuel, V. T., Miller, P., Previs, S. F., Suino-Powell, K., Xu, H. E., Shulman, G. I., Kliewer, S. A., and Mangelsdorf, D. J. (2011) FGF19 as a postprandial, insulin-independent activator of hepatic protein and glycogen synthesis. *Science* **331,** 1621–1624
17. Potthoff, M. J., Boney-Montoya, J., Choi, M., He, T., Sunny, N. E., Satapati, S., Suino-Powell, K., Xu, H. E., Gerard, R. D., Finck, B. N., Burgess, S. C., Mangelsdorf, D. J., and Kliewer, S. A. (2011) FGF15/19 regulates hepatic glucose metabolism by inhibiting the CREB-PGC-1alpha pathway. *Cell Metab.* **13,** 729–738
18. Huang, X., Yang, C., Luo, Y., Jin, C., Wang, F., and McKeehan, W. L. (2007) FGFR4 prevents hyperlipidemia and insulin resistance but underlies high-fat diet induced fatty liver. *Diabetes* **56,** 2501–2510
19. Thomas, C., Pellicciari, R., Pruzanski, M., Auwerx, J., and Schoonjans, K. (2008) Targeting bile-acid signalling for metabolic diseases. *Nat. Rev. Drug Discov.* **7,** 678–693
20. Kobayashi, M., Ikegami, H., Fujisawa, T., Nojima, K., Kawabata, Y., Noso, S., Babaya, N., Itoi-Babaya, M., Yamaji, K., Hiromine, Y., Shibata, M., and Ogihara, T. (2007) Prevention and treatment of obesity, insulin resistance, and diabetes by bile acid-binding resin. *Diabetes* **56,** 239–247
21. Lundåsen, T., Andersson, E. M., Snaith, M., Lindmark, H., Lundberg, J., Östlund-Lindqvist, A. M., Angelin, B., and Rudling, M. (2012) Inhibition of intestinal bile acid transporter Slc10a2 improves triglyceride metabolism and normalizes elevated plasma glucose levels in mice. *PLoS One* **7,** e37787
22. Yu, X. X., Watts, L. M., Manchem, V. P., Chakravarty, K., Monia, B. P., McCaleb, M. L., and Bhanot, S. (2013) Peripheral reduction of FGFR4 with antisense oligonucleotides increases metabolic rate and lowers adiposity in diet-induced obese mice. *PLoS One* **8,** e66923
23. Cyphert, H. A., Ge, X., Kohan, A. B., Salati, L. M., Zhang, Y., and Hillgartner, F. B. (2012) Activation of the farnesoid X receptor induces hepatic expression and secretion of fibroblast growth factor 21. *J. Biol. Chem.* **287,** 25123–25138